Curvature radiation and giant subpulses in the Crab pulsar

Janusz Gil[1] & George I. Melikidze[1,2]

ABSTRACT

It is argued that the nanosecond giant subpulses detected recently in the Crab pulsar are generated by means of the coherent curvature radiation of charged relativistic solitons associated with sparking discharges of the inner gap potential drop above the polar cap.

Subject headings: pulsars: giant pulses - pulsars: individual (Crab pulsar)

1. Introduction

Although only four pulsars are known to emit giant pulses (Lundgren et a. 1995; Cognard et al. 1996; Romani & Johnston 2001; Johnston & Romani 2003), understanding the mechanism of their radiation can potentially lead to understanding the longstanding problem of a pulsar radio emission. Recently, the detection of extremely short and powerful, 2-nanosecond - 1000 Jy, subpulses within the radio giant pulses from the Crab pulsar has been reported by Hankins et al. (2003, HKWE03 hereafter). This is an observational result of extraordinary importance, for it can shed a new light onto the mystery od coherent pulsar radio emission. HKWE03 argued that these nanosecond giant subpulses were true temporal modulations associated with an explosive collapse of nonlinear plasma turbulence (Weatherall et al. 1998). In this letter we argue that the time-scale of the Crab pulsar giant nanosecond subpulses is consistent with the angular beaming due to the curvature of dipolar field lines (different from the conventional angular beaming due to the pulsar rotation), thus with the coherent curvature radiation. Furthermore, we demonstrate that the observed fluxes of these giant subpulses are consistent with the emission of charged relativistic solitons, generated by means of the modulational instability of the strong Langmuir turbulence associated with a sparking discharge of the pulsar's polar gap (Melikidze, Gil & Pataraya 2000, MGP00 hereafter; Gil, Lyubarski & Melikidze 2004, GLM04 hereafter).

[1]Institute of Astronomy, University of Zielona Góra, Lubuska 2, 65-265, Zielona Góra, Poland

[2]Abastumani Astrophysical Observatory, Al.Kazbegi ave. 2a, Tbilisi 0160, Georgia

2. The time-scales

2.1. The Alignment Time-scale

Let us consider a number of localized (point-like) sources of the broadband coherent curvature radiation, moving relativistically (with the Lorentz factor $\gamma = (1-\beta^2)^{-1/2}$, where $\beta = v/c \sim 1$) along a narrow bundle of dipolar magnetic field lines with a radius of curvature

$$\rho = 1.8 r_6^{1/2} s^{-1} 10^7 \text{ cm}, \tag{1}$$

where $s = d/r_p$ is the normalized polar coordinate of the central line of the bundle, $r_6 = r_{\rm em}/R$ is the normalized emission altitude r (for the frequency $\nu = 5$ GHz, $5 < r_6 < 35$ in the Crab pulsar, Kijak & Gil 1998), d is the distance from the dipolar axis to the foot of a dipolar field line, $r_p \approx 10^4 P^{-1/2}$ is the polar cap radius and $R = 10^6$ cm is the neutron star radius. The geometry is schematically illustrated in Fig. 1 where a narrow bundle of field lines is marked. The curvature radiation is emitted along dipolar field lines into a narrow cone with an opening angle $\theta = 1/\gamma$ (e.g. Jackson 1975). In what follows we assume that the perpendicular dimension of each source measured by the angular extent of the bundle of field lines does not exceed θ (validity of this assumption is justified later on in the paper). We also assume that other bundles carrying sources of coherent curvature radiation are separated by at least θ, thus only one narrow bundle contributes to the radiation observed at a given rotational phase $\varphi = 2\pi t/P$, where t is the intrapulse time. For a fixed arrangement of the observer's direction, the field line polar coordinate s and the frequency dependent emission altitude $r_6(\nu)$, each source is aligned within $1/\gamma$ with the observer during the time interval $\delta t = l/v = \rho\theta/v = \rho\gamma^{-1}/v$ (see Fig. 1), where ρ is described by equation (1). Therefore, a continuous stream of relativistic sources moving along a curved trajectory would illuminate the observer during the time interval

$$\Delta t = \rho\gamma^{-1}/c \ , \tag{2}$$

provided that this "alignment" time-scale is longer than the conventional angular beaming time scale $\Delta t' = \gamma^{-1} P/2\pi$ related purely to the pulsar rotation. In the case of the Crab pulsar this means that $\rho > 1.6 \times 10^8$ cm in the case of the Crab pulsar. HKWE03 concluded that the conventional angular beaming cannot explain the 2-nanosecond duration of their giant subpulses, since it indeed requires $\gamma \sim 10^6$, much above the expected values $\gamma < 1000$. Since, incidentally, in the case of the Crab pulsar $\Delta t' \sim \Delta t$, their conclusion applies also to the alignment time scale related to the field line curvature (eq.[2]).

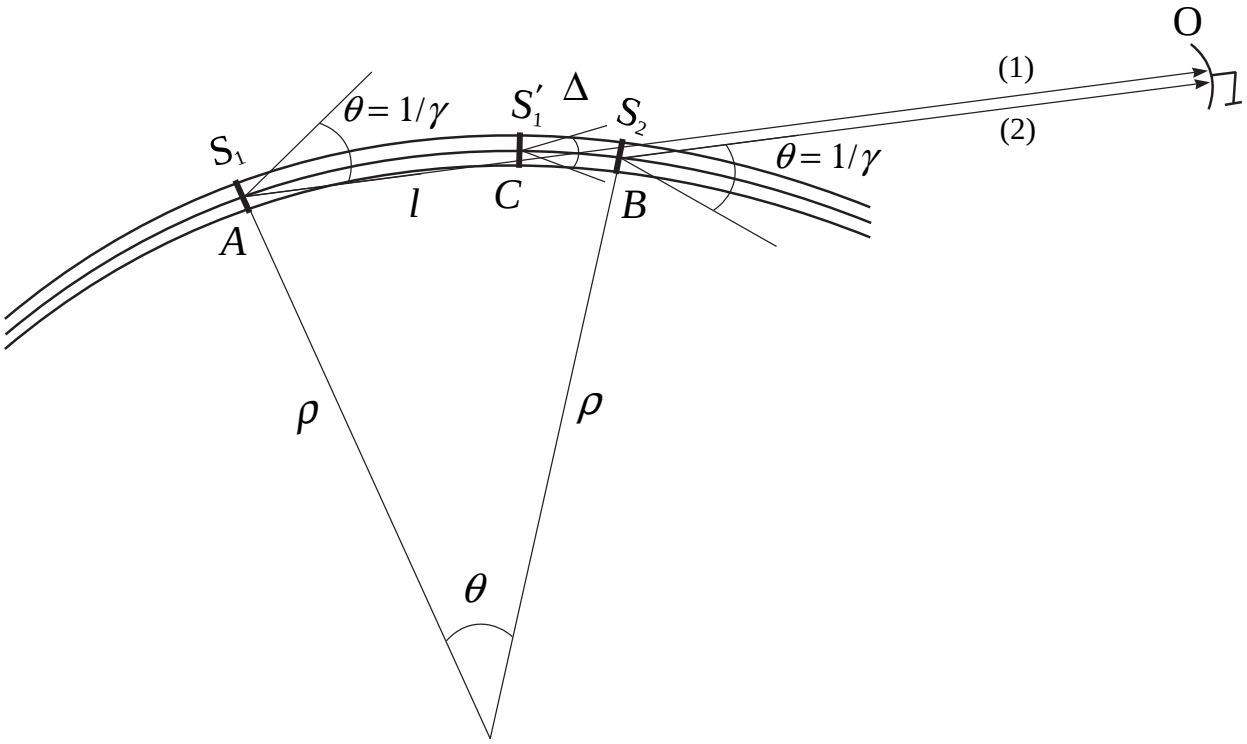

Fig. 1.— Geometry of the observed curvature radiation emitted by the source (S) moving relativistically along a narrow bundle od dipolar field lines with the radius of curvature ρ (see text for explanation of other symbols).

2.2. The Apparent Time-Scale

The situation can be quite different if the stream is not continuous but some sources are distinguished by emitting slightly more power $\mathcal{P}$ than the average. From the observational point of view it means that there are very few sources emitting towards the observer. For simplicity let us first consider a single source, which is marked in Fig. 1 in three different positions A, B and C. Following Jackson (1975) we can argue that the duration of the observed impulse related to the curvature of field lines is much shorter than that predicted by equation (2). Let us consider two particular points along a given dipolar field line: first (A) at which the source S_1 becomes aligned (ray 1) and second (B) at which it becomes misaligned (ray 2) with the observer O (Fig.1). The source covers a distance $l = \rho/\gamma$ between these points during a time interval $\delta t = \rho\gamma^{-1}/v$. During this time the radiation emitted at the first alignment point (A) travels a distance $L = c\delta t = (c/v)\rho\gamma^{-1} = \rho/(\beta\gamma)$. Thus, the radiation overtakes the source only by a distance $\Delta = L - l = (1/\beta - 1)(\rho/\gamma) \approx \rho/\gamma^3$ (when the radiation emitted at point A reaches point B, the source of this radiation arrives at point C). This is the pulse length in space, and thus the duration of the observed impulse emitted by the considered source is

$$\Delta\tau = \frac{\Delta}{c} = \frac{\rho}{c\gamma^3} = \gamma^{-2}\Delta t \ , \tag{3}$$

(Gil 1985) where Δt is the alignment time scale (eq.[2]). Therefore, if the longitudinal (along field lines) source dimension is smaller than $\Delta \approx \rho/\gamma^3$, then the apparent duration of the impulse $\Delta\tau$ is γ^2 times shorter than the actual time of alignment of the source with the observer. It is important to emphasize that this apparent shortening effect has nothing to do with special relativity (time dilation) and/or Doppler effects, as both Δt and $\Delta\tau$ are referred to the same observer's frame. This effect occurs for any localized source of emission (radiation, particles, etc.) moving towards the observer (target) with a speed slightly lower that the emitted waves (particles). For example, one can consider an acoustic analog in which a highly directional loud-speaker is moving along a curved trajectory with a velocity close to the speed of sound. The duration of the acoustic impulse is much shorter than the actual time of geometrical alignment of the beam pattern with the recording device. The acoustic analog of equation (3) is $\Delta\tau = \Theta^2\Delta t$, where Θ is the beam-width of the emitted pattern (in radians).

Both isolated 2-ns giant subpulses, as well as a sequence of a number of such subpulses (when unresolved this sequence constitutes a normal giant pulse in our view), can be seen in Fig. 1 of HKWE03. Within our model such case corresponds to a sequence of sources, each having a longitudinal dimension smaller than Δ and separation between the adjacent sources larger than Δ, where $\Delta \approx \rho/\gamma^3$ is the spatial length of the impulse associated with each source. For each giant subpulse detected by HKWE03 the observed time duration

$\Delta\tau = 2 \times 10^{-9}$ s (eq.[3]), which leads to the condition

$$\rho_8 \approx 0.6\gamma_2^3 \ , \tag{4}$$

where $\rho_8 = \rho/10^8$ cm (eq.[1]) and $\gamma_2 = \gamma/10^2$.

3. Energetics

3.1. Brightness Temperature

As reported by HKWE03, the ultra-short nano-giant subpulses detected at $\nu = 5$ GHz in the Crab pulsar often exceed fluxes $S = 1000$ Jy $= 10^{-20}$erg s^{-1}Hz^{-1}cm^{-1}. These fluxes can be converted into the brightness temperature $T_b = SD^2/[2k(\nu W)^2]$, where $D = 2$ kpc $= 6 \times 10^{21}$cm is the distance to the pulsar, k is the Boltzmann constant and W is the time scale of the corresponding emission process (e.g. McLaughlin and Cordes 2003). Assuming that $W = 2 \times 10^{-9}$s (HKWE03) one obtains the extraordinarily high brightness temperatures $T_b \sim 10^{38}$K, implying by far the most luminous emission from any astronomical object. However, within our model the actual emission process corresponding to a giant subpulse of duration $\Delta\tau = 2 \times 10^{-9}$s occurs over a much longer "alignment" time interval $W = \Delta t = \gamma^2\Delta\tau$ (eqs. [2] and [3]), which leads to γ^4 times lower brightness temperatures. Since γ is of the order of 100, then $T_b < 10^{30}$ K, consistent with normal giant pulses in the Crab pulsar and other pulsars (see Fig. 1 in McLaughlin and Cordes, 2003).

3.2. Luminosity and Power

Let us then consider a source(s) moving along a dipolar field line (Fig. 1) and emitting a coherent curvature radiation with an intrinsic power $\mathcal{P}$. While moving over the alignment distance $l = \rho\gamma^{-1}$, the emitted energy $E = \mathcal{P}\Delta t$, where the alignment time interval $\Delta t = \rho\gamma^{-1}/c$ (eq.[2]). This energy is received by the observer in a much shorter time $\Delta\tau = \gamma^{-2}\Delta t$ (eq.[3]), and therefore the apparent luminosity

$$\mathcal{L} = \frac{E}{\Delta\tau} = \gamma^2\mathcal{P}. \tag{5}$$

Thus, the nanosecond giant subpulses appear $\gamma^2 = \gamma_2^2 10^4$ more luminous than the intrinsic power of their source(s). Also the apparent fluxes $S \propto \mathcal{L}$ are γ^2 times overestimated. It is important to emphasize that this kinematical boosting is a direct consequence of an apparent shortening of the impulse duration described by equation (3) and again has nothing to do

with special relativity and/or Doppler effects (Ginzburg 1979). According to the discussion below equation (3), an acoustic analog of equation (5) is $\mathcal{L} = \Theta^{-2}\mathcal{P}$.

The apparent fluxes $S \sim 1000$ Jy of the nanosecond giant subpulses can be formally converted into the emitted luminosity $\mathcal{L} = S\theta^2 D^2 \Delta\nu$. With $D = 2$ kpc, $\theta = \gamma_2^{-1}10^{-2}$ and $\Delta\nu \sim 10^9$ Hz one obtains $\mathcal{L} \sim \gamma_2^{-2}10^{28}$ erg/s. This is an extremely large value, comparable with the total radio luminosity of the Crab pulsar $L_R = 3.5 \times 10^{25+x}$ erg s^{-1}, where $x = logL \approx 3.6$ mJy kpc^2 from the Pulsar Catalog (Taylor, Manchester & Lyne 1993). The existence of such powerful localized sources of coherent radio emission seems highly questionable (of course, this argument is not independent from the extraordinarily high brightness temperatures $T_b \sim 10^{38}$K derived in Section 3.1). However, according to equation (5), the actual power of the emitted radiation $\mathcal{P} = \gamma^{-2}S\theta^2 D^2 \Delta\nu = \gamma^{-2}\mathcal{L}$, which for the parameters given above yields approximately

$$\mathcal{P} \sim \gamma_2^{-4}10^{24} \text{ erg s}^{-1}. \tag{6}$$

This is still a very large power (consistent with $T_b \lesssim 10^{30}$ K) but much smaller than the total radio luminosity of the Crab pulsar. In the next section we discuss a mechanism of coherence of the curvature radiation that can produce shots of radio emission of nanosecond duration with the intrinsic power corresponding to the values described by equation (6).

Finally we can check whether our localized source can be supplied with enough kinetic energy to emit giant subpulses. To estimate the energy of the source let us note that the product of plasma number density and the cross-section of the corresponding flux tube is a constant value equal to $\kappa n_{\rm GJ} h^2$, where $n_{\rm GJ}$ is the Goldreich & Julian (1969) density, κ is the Sturrock (1971) multiplication factor and h is the gap height (equal to the spark size). Assuming that the perpendicular source dimensions are determined by the spark size, we can write that the kinetic energy associated with the source is $E_{\rm sr} \approx n_{\rm GJ}\kappa mc^3 h^2 \Delta/c$. On the other hand, the giant subpulse energy $E_{\rm GP} = \gamma^2 \mathcal{P}\Delta\tau = \gamma^2\mathcal{P}\Delta/c$ (eqs.[3] and [5]). Obviously $E_{\rm GP}$ should be smaller than $E_{\rm sr}$, which leads to the condition $\kappa\gamma_2^3 > 500$, consistent with an independent estimate given by GLM04.

4. Coherent curvature radiation

MGP00 proposed a model for generation of the coherent pulsar radio emission, based on the idea of the polar gap discharging via a number of localized sparks (Ruderman & Sutherland 1975). The sparking phenomenon creates a succession of plasma clouds moving along dipolar magnetic field lines. The overlapping of charged particles with different energies from the adjacent clouds ignites a strong Langmuir turbulence via the two-stream instability

(Usov 1987; Asseo & Melikidze 1998). In the pulsar magnetospheric conditions, this turbulence is subject to modulational instability, which leads to the formation of "bunch-like" charged solitons capable of generating the coherent curvature emission at radio-wavelengths λ. Thus, the condition $\lambda < \Delta = \rho/\gamma^3 = (\rho_8/\gamma_2^3)10^2$ is naturally satisfied at centimeter wavelengths (note that according to eq.[4] $\Delta = 60$ cm, which of course corresponds to 2 light nanoseconds). Additionally, the angular extent $\Delta\psi$ of the bundle of dipolar field lines associated with a given spark should not exceed $\theta = \gamma^{-1}$. It is easy to show that in the Crab pulsar $\Delta\psi \sim 0.001 < \gamma^{-1}$ (for details see Gil & Sendyk 2000).

MGP00 calculated the power of the soliton curvature radiation in the vacuum approximation, that is without taking into account the influence of the magnetospheric plasma. GLM04 reconsidered the curvature radiation of a point-like charge moving through electron-positron plasma. They demonstrated that the radiation power is suppressed by a factor of about $10^{-2} - 10^{-3}$ but still at a high enough level to explain the observed pulsar luminocities. Applying the results of MGP00 modified by GLM04 to the case of the Crab pulsar, we obtain that the power radiated by one soliton can be as high as $L_1 \sim 10^{21}$ erg/s. Thus, for an incoherent superposition of N sources of the coherent radio-emission (solitons), each smaller than Δ and separated from each other by more than Δ, we have

$$L \sim N10^{21} \text{ erg/s}, \tag{7}$$

(for details see eqs. [14] - [18] in MPG00). Comparing equation (7) with the power required for the Crab giant subpulses expressed by equation (6) one obtains the Lorentz factors $\gamma_2 \gtrsim 10^{3/4}/N^{1/4}$, which is realistically about 3-4 (consistent with an independent estimate for $\gamma \sim 300 - 400$ given by GLM04). Inserting $\gamma_2 = 3$ into equation (4) we obtain $\rho_8 \gtrsim 16$, which, according to equation (1), means $r_6^{1/2} s^{-1} \sim 90$. Since $r_6 < 35$ (Kijak & Gil 1998) this implies that $s < 0.07$. Remembering that s is a normalized polar coordinate (0 - for the pole and 1 for the polar cap edge), we conclude that only those field lines that originate very close to the magnetic axis can be involved with the nanosecond giant sub-pulses. Such field lines can be aligned with the observer in the radio emission region only within a very narrow range of longitudes near the so-called fiducial plane, containing both the spin and magnetic axes. It is natural to associate this plane with the peak of the pulse profile. Thus, within our model, the giant subpulses should occur only within a very narrow range of longitudes near the peak of the radio profile. To the best of our knowledge, giant subpulses in the Crab pulsar seem to occupy the narrow range of phases within about 1% of the pulse window near the peak of the main-pulse (HKWE03). This is consistent with the phase range $2\psi/360^\circ = s(2.^\circ4/360^\circ)(r_6/P)^{1/2}$, which for $s < 0.07$ and $r_6 < 35$ (see above) is smaller than 0.015.

5. Discussion

In this letter we argue that the 2-ns giant subpulses detected in the Crab pulsar are due to the curvature radiation of one or at most several solitons associated with a sparking discharges occurring near the local surface magnetic pole. This is the most elementary emission event that can be observationally resolved. The curvature radiation from the particular soliton(s) can be observationally distinguished by means of the kinematical boosting (eq.[3]) only if they are slightly more powerful than other solitons. This implies that the sparking event associated with giant subpulses is more energetic than an average one. Both luminosity and characteristic frequency of the soliton curvature radiation strongly depend on the Lorentz factor γ, which in turn depends on the accelerating potential drop above the polar cap. Interestingly, pulsars exhibiting giant pulses are distinguished not only by their brightness, but also by extremely high values of the so-called complexity parameter $a = (r_p/h)$, where r_p is the polar cap radius and h is the polar gap height (Gil & Sendyk 2000). Since the accelerating potential drop $\Delta V \propto h^2$ and $h < r_p/\sqrt{2}$ (Ruderman & Sutherland 1975), then pulsars with very high values of $a >> 1$ must have a large reservoir of the maximum available potential drop over the actual potential drop ($\Delta V_{max}/\Delta V = a^2/2$). This reservoir can be occasionally used to create exceptionally energetic spark(s).

The values of the complexity parameter a can well exceed 100 in normal pulsars, while in millisecond pulsars they are limited to about 40 (see Fig. 1 in Gil & Sendyk 2000). Therefore, when pulsars in both groups are ranked with respect to a, pulsars with giant pulses occupy the top of the lists (Table 1). Also, the Vela pulsar, which was reported to exhibit some kind of giant pulse behavior (Johnston et al. 2001) is very high on the list. Moreover, sporadic large amplitude pulses (LAP) from two millisecond pulsars (J1959+2048 and J0218+4232) have been reported very recently by Joshi et al. (2003). It should be emphasized that pulsars showing giant pulses have also high values of the magnetic field $B_{\rm LC} \gtrsim 10^5$ G at the light cylinder. This might, however, be a coincidence because roughly $B_{\rm LC} \sim a^2/P$, where P is the pulsar period (Table 1). Although $B_{\rm LC}$ is a good parameter to make a list of giant pulse candidates, only a value of a^2 has a physical meaning within our model. In Table 1 we propose a number of candidates for giant pulses with high values of the complexity parameter ($a > 10$ for millisecond pulsars and $a > 90$ for normal pulsars) and relatively low values of $B_{\rm LC}$. The detection (non-detection) of giant pulses from these candidates would confirm (refute) our scenario. PSR J1119-6127 with low $B_{\rm LC} \approx 5 \times 10^3$ G seems the most interesting case.

The case of PSR J1959+2048 deserves some additional discussion in the light of the model discussed here. As emphasized by Johnston & Romani (2003), this pulsar is exceptional in the sense that despite the high value of $B_{\rm LC}$ it does not show giant emission

Table 1. Pulsar parameters

PSR J	P (msec)	$\dot{P}$ (10^{-15})	a	B_{LC} (10^5G)	
0534+2200	34	420	249	8.7	(2)
0540−6919	51	479	198	3.3	(6)
1513−5908	150	1540	138	0.4	(21)
1124−5916	135	745	120	0.4	(22)
1617−5055	69	137	114	0.8	(12)
1420−6048	68	83	99	0.7	(14)
1119−6127	408	4002	95	0.05	(75)
0835−4510	89	125	94	0.4	(20)
1824−2452	3	0.0016	33	7.3	(4)
1823−30A	5.4	0.0034	28	2.4	(8)
1939+2134	1.6	0.0001	23	8.8	(1)
0218+4232	2.3	0.00007	16	3.1	(7)
1959+2048	1.6	0.00002	14	3.6	(5)
2129+1210E	4.6	0.00018	14	8.2	(3)

Note. — Pulsars marked in boldface show giant pulses, others are candidates for giant pulse emission. Numbers in parenthesis denote ranking position in $B_{LC} = 2850\dot{P}^{0.5}P^{-2.5}$. The complexity parameter $a = 425(\dot{P})^{2/7}P^{-9/14}$.

(although Joshi et al. (2003) found one significant LAP (out of million pulses) with an intensity 129 times the mean intensity). This seems to be consistent with our model since this pulsar (which is fourth ranked with respect to $B_{\rm LC}$) has a relatively small value of the complexity parameter a as compared with two other millisecond pulsars showing giant pulses (Table 1). In fact, since $\Delta V_{\rm max}/\Delta V = a^2/2$, the smaller the value a, the smaller the reservoir of the polar gap energy that can ignite giant emission.

Also the case of Vela pulsar is very interesting in view of the models of giant emission. Kramer, Johnston & van Straten (2002) reported giant micro-pulses in this pulsar, which are different from normal micro-pulses and are probably closely related to classical giant pulses. They have typically large amplitudes, appear to be narrower than normal micro-pulses and exhibit a power law in their cumulative probability distribution. The first two properties are quite natural within our model (a sequence of unresolved nano-pulses?) and we discuss the last issue bellow.

According to our scenario, both ordinary and giant pulses are related to the inner gap sparking activity and originate at relatively low altitudes, contrary to the suggestion that the latter arise in the outer gap region (Romani & Johnston 2001). Generally, the following two steps are involved: first a corresponding spark should be relatively intense (which corresponds to relatively high Lorentz factors), so the associated solitons are distinguished from the background radiation (the soliton radiation intensity depends very strongly on the Lorentz factor, see eq.[43] in GLM04). Then, in the second step, the intensity of the curvature radiation of distinguished soliton(s) can be kinematically boosted by means of equation (5). It is intuitive that the distribution of spark energy is quasi-gaussian, with a low energy cutoff corresponding to the pair formation threshold. Since the giant pulses should be associated with sparks corresponding to the high energy tail of this distribution, it is natural that they exhibit a power law in their cumulative probability distribution.

This paper is supported in part by the Grant 2 P03D 008 19 of the Polish State Committee for Scientific Research. We thank D. Melrose and Q. Luo for their hospitality and fruitful discussions during our stay at the School of Physics Sydney University. We thank E. Gil and U. Maciejewska for technical help.

REFERENCES

Asseo, E., & Melikidze, G. I. 1998, MNRAS, 301, 59

Cognard, L., Shrauner, J.A., Taylor, J.H. & Thorsett, S.E., 1996, ApJ, 457, L81

Gil, J., 1985, A&A 143, 443-446

Gil, J., Lyubarsky, Y., & Melikidze, G.I. 2004, ApJ, in press (GLM04), astro-ph/0310621

Gil, J. & Sendyk, M. 2000, ApJ, 541, 351

Ginzburg, V.L. 1979, Theoretical physics and Astrophysics, sec. 5, Pergamon Press, Oxford

Goldreich, P., & Julian, H. 1969, ApJ, 157, 869

Hankins, T.H., Kern, J.S., Weatherall, J.C. & Eilek, J.A. 2003, Nature, 422, 141 (HKWE03)

Jackson, J. D. 1975, Classical electrodynamics, John Wiley & Sons, NY

Johnston, S., & Romani, R.W. 2003, astro-ph/0305235

Johnston, S., et al. 2001, ApJ, 549, L101

Joshi, B.C. et al. 2003, astro-ph/0301285

Kramer, M., Johnston, S., & van Straten, W. 2002, MNRAS. 334, 523

Kijak, J., & Gil, J. 1998, MNRAS, 299, 855

Lundgren, S.C., et al., ApJ, 453, 433

McLaughlin, M.A., & Cordes, J.M. 2003, astro-ph/0304365

Melikidze, G. I, Gil, J., & Pataraya, A. D. 2000, ApJ, 544, 1081 (MGP00)

Romani, R.W., & Johnston, S. 2001, ApJ, 557, L93

Ruderman, M. A., & Sutherland, P. G. 1975, ApJ, 196, 51

Sturrock, P. A. 1971, ApJ, 164, 529

Taylor, J.H., Manchester, R.N., & Lyne, A.G. 1993, ApJS, 88, 259

Usov, V. V. 1987, ApJ, 320, 333

Weatherall J.C. 1998, ApJ, 506, 341